Plant Physiology and Biochemistry 143 (2019) 275–285

Contents lists available at ScienceDirect

Plant Physiology and Biochemistry

journal homepage: www.elsevier.com/locate/plaphy

Research article

Silicon alleviates the impairments of iron toxicity on the rice photosynthetic performance via alterations in leaf diffusive conductance with minimal impacts on carbon metabolism

Martielly S. dos Santos[1], Lílian M.P.V. Sanglard[2], Samuel C.V. Martins, Marcela L. Barbosa, Danilo C. de Melo, William F. Gonzaga, Fábio M. DaMatta*

Departamento Departamento de Biologia Vegetal, Universidade Federal de Viçosa, 3570-900, Viçosa, MG, Brazil

ARTICLE INFO

Keywords:
photosynthesis
Iron toxicity
Oryza sativa
Silicon

ABSTRACT

Iron (Fe) toxicity is often observed in lowland rice (*Oryza sativa* L.) plants, disrupting cell homeostasis and impairing growth and crop yields. Silicon (Si) can mitigate the effects of Fe excess on rice by decreasing tissue Fe concentrations, but no information exists whether Si could prevent the harmful effects of Fe toxicity on the photosynthesis and carbon metabolism. Two rice cultivars with contrasting abilities to tolerate Fe excess were hydroponically grown under two Fe levels (25 μM or 5 mM) and amended or not with Si (0 or 2 mM). Fe toxicity caused decreases in net photosynthetic rate (A), particularly in the sensitive cultivar. These decreases were correlated with reductions in stomatal (g_s) and mesophyll (g_m) conductances, as well as with increasing photorespiration. Photochemical (e.g. electron transport rate) and biochemical (e.g., maximum RuBisCO carboxylation capacity and RuBisCO activity) parameters of photosynthesis, and activities of a range of carbon metabolism enzymes, were minimally, if at all, affected by the treatments. Si attenuated the decreases in A by presumably reducing the Fe content. In fact, A as well as g_s and g_m, correlated significantly with leaf Fe contents. In summary, our data suggest a remarkable metabolic homeostasis under Fe toxicity, and that Si attenuated the impairments of Fe excess on the photosynthetic apparatus by affecting the leaf diffusive conductance with minimal impacts on carbon metabolism.

1. Introduction

Iron (Fe) is a micronutrient that plays a crucial role in plant metabolism, as denoted by its functions in redox reactions of photosynthesis, respiration and nitrogen assimilation (Ricachenevsky et al., 2010; Vigani et al., 2013). However, when in excess, Fe is associated with increased production of reactive oxygen species, via Fenton and Haber-Weiss reaction (Onaga et al., 2016), which ultimately leads to morphophysiological disorders, including cell damages with degradation of cell membranes (Pereira et al., 2013), nutritional disorders (Müller et al., 2015), iron plaque formation in roots (Pereira et al., 2014; Pinto et al., 2016) and decreased photosynthetic performance, thus impairing growth and crop yields (Audebert and Fofana, 2009; Stein et al., 2009). Disruption of carbon metabolism is due mostly to feedback inhibition by ATP and NADPH which are not properly used in the Calvin-Benson cycle under Fe excess (Siedlecka et al., 1997).

Iron toxicity is a major mineral disorder in lowland rice production (Audebert and Fofana, 2009) due to excess ferrous iron (Fe^{2+}) formation under acid and anoxic soil conditions. This toxicity can be direct, caused by excessive metal accumulation, or indirect, due to decreased uptake of nutrients such as P, K, Ca and Mg (Silveira et al., 2007; Stein et al., 2009; Müller et al., 2015). Regardless, Fe toxicity has been shown to disrupt rice photosynthetic activity coupled with decreased productivity, which depends on the tolerance of the cultivar, severity and time of stress imposition (Stein et al., 2009, 2014). Decreases in the net CO_2 assimilation rate (A) under Fe toxicity have been attributed to impairments in photochemical reactions as well as to stomatal and non-stomatal limitations of photosynthesis (Pereira et al., 2013; Pinto et al., 2016). In addition to stomatal conductance (g_s), which is related to the diffusion of CO_2 from the surrounding atmosphere to the intercellular air spaces, the photosynthetic capacity is also influenced by mesophyll conductance (g_m), which in turn is related to the diffusion of CO_2 from

* Corresponding author.
E-mail address: fdamatta@ufv.br (F.M. DaMatta).
[1] Present address: Departamento de Ciências Biológicas, Universidade Estadual de Santa Cruz, Rodovia Jorge Amado km 16, Ilhéus, BA, Brazil
[2] Present address: Australian Research Council Centre of Excellence in Plant Energy Biology, University of Western Australia, Crawley, WA, 6009, Australia

https://doi.org/10.1016/j.plaphy.2019.09.011
Received 10 July 2019; Received in revised form 9 August 2019; Accepted 5 September 2019
Available online 11 September 2019
0981-9428/

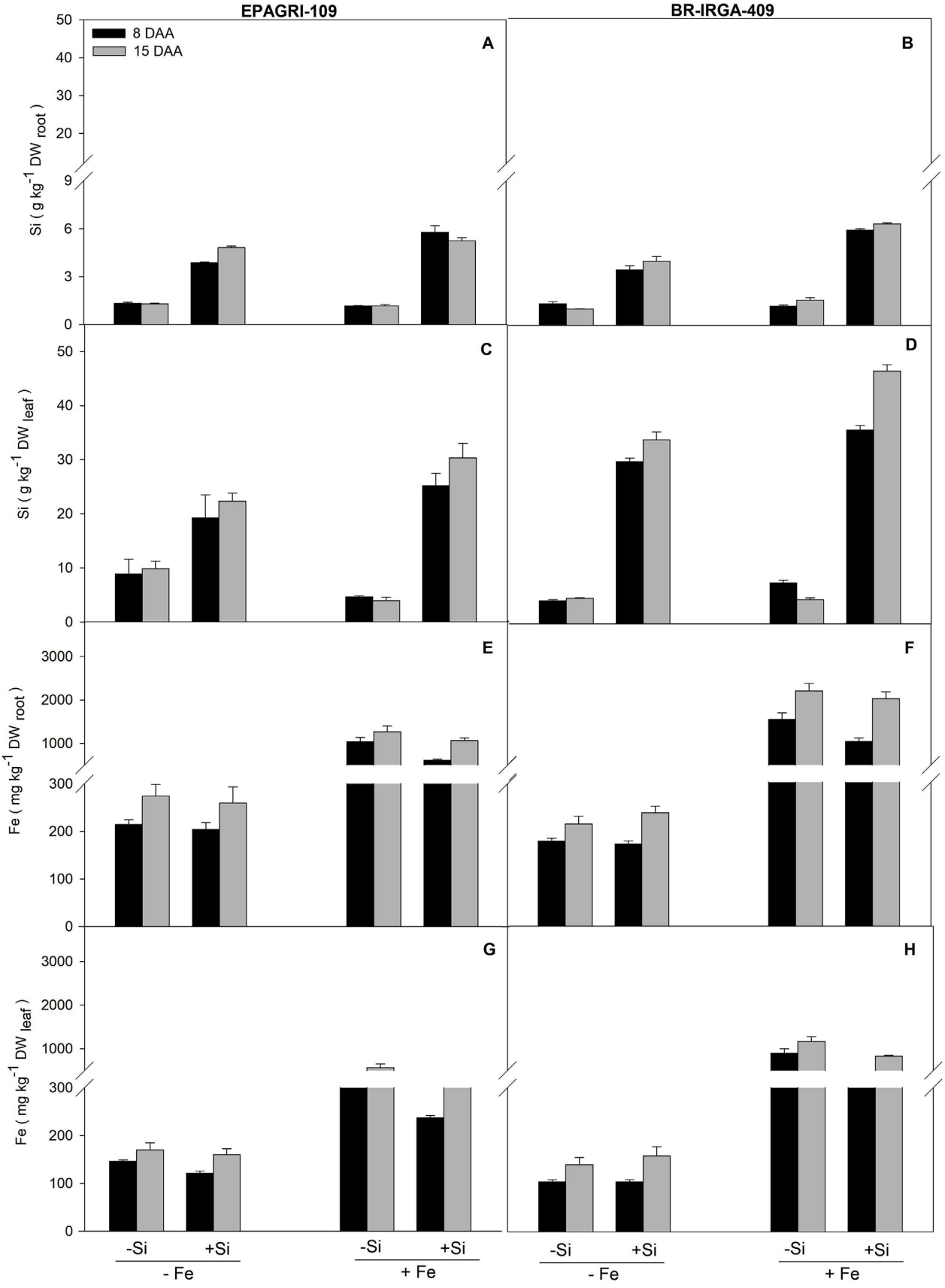

Fig. 1. The effects of silicon, Si (0 or 2 mM: Si or + Si, respectively), and iron, Fe (25 μM or 5 mM: Fe and +Fe, respectively), on the root and leaf concentrations of Si (A–D) and Fe (E–H) of two rice cultivars [cv. 'EPAGRI-109' and cv. 'BR-IRGA-409', respectively tolerant and sensitive to Fe excess] grown in nutrient solutions. The measurements were performed at 42 days after applying Fe excess. n = 5 ± SE.

Table 1
The results (significance: ^{ns} not significant, $*P < 0.05$, $**P < 0.01$, $***P < 0.001$) of ANOVA for the effects of silicon (Si), iron (Fe) and cultivar (Cv) and their interactions on root and leaf concentrations of Si and Fe, net CO_2 assimilation rate (A), stomatal conductance (g_s), mesophyll conductance (g_m), stomatal (SL), mesophyll (ML) and biochemical (BL) limitations of photosynthesis, maximum rate of RuBisCO carboxylation on a chloroplast basis (V_{cmax}), maximum rate of carboxylation limited by electron transport (J_{max}), ratio of electron transport rate devoted to oxygenation/carboxylation (J_o/J_c), variable-to-maximum Chl fluorescence ratio (F_v/F_m), efficiency of the capture of excitation energy by open photosystem II reaction centres (F_v'/F_m'), and photochemical quenching coefficient (q_P), nucleotide ratios, carbohydrates, malate, fumarate and proteins. The results are present in the form of y/y, i.e. at 8 or 15 days after Fe additions. When a single result is presented, it represents the same significance for both days.

Parameters	Si	Fe	Si x Fe	Cv	Si x Cv	Fe x Cv	Si x Fe x Cv
Leaf Si	***	***/**	***	ns	ns	ns/***	ns
Root Si	***	*/**	**/***	***	ns/***	ns/*	ns
Leaf Fe	*/**	***	*/**	***	ns	***	ns
Root Fe	***	***	***	***	*/ns	***	**/*
A	***	***	*	ns/**	ns	ns/**	ns
g_s	***	***	*/ns	*/ns	ns	***/*	ns
g_m	***/ns	***	ns	ns	ns	ns	ns
LS	**/***	***	ns	*/ns	ns	**/*	ns
LM	***/ns	***	***/*	ns/**	*/ns	ns/***	**/ns
LB	***	***	***	ns/***	ns	*	ns/**
V_{cmax}	ns	ns	ns	**/ns	ns/*	ns	ns
J_{max}	ns/***	ns/*	ns/*	ns/***	ns	ns	ns
J_o/J_c	**/***	***	*	ns	ns	***/*	ns
F_v/F_m	ns	ns	ns/*	**/ns	ns	ns	ns/*
F_v'/F_m'	ns/*	***	**	ns	ns/*	ns	ns
q_p	ns	ns/**	ns	ns	ns	ns	ns
NADH/NAD$^+$	ns	***	ns	ns	ns	***	ns
NADPH/NADP$^+$	**	***	ns	**	*	ns	ns
Glucose	***	***	**	***	ns	***	**
Fructose	**	***	***	***	ns	ns	*
Sucrose	ns	ns	ns	ns	ns	ns	ns
Starch	ns	ns	ns	ns	ns	ns	ns
Malate	***	***	ns	****	***	ns	ns
Fumarate	***	***	ns	****	*	ns	ns
Proteins	ns	ns	ns	ns	ns	ns	ns

the intercellular spaces to the carboxylation sites in the chloroplast stroma (Flexas et al., 2012). So far, the effects of Fe toxicity on g_m are virtually unknown, although the effects of other toxic metals on g_m have been reported (Sagardoy et al., 2010; Velikova et al., 2011; Sanglard et al., 2014).

Although silicon (Si) is not recognized as an essential element for plant growth, there seems to be no doubts that it can be beneficial in protecting plants against stresses, biotic and abiotic, even though the underlying mechanisms affording such protection remain unresolved (Debona et al., 2017; Coskun et al., 2019). Some negative effects associated with metal/metalloid toxicity, including e.g. aluminium (Liang et al., 2001), arsenic (Sanglard et al., 2016), boron (Gunes et al., 2007), cadmium (Shi et al., 2010), manganese (Li et al., 2012) and zinc (Neumann and zur Nieden, 2001), have been alleviated or prevented by proper Si fertilization. In the case of Fe toxicity in particular, some information suggests that Si can mitigate the effects of toxicity on rice via decreased Fe concentrations in both leaf and root tissues, increased activity of the antioxidant system with concomitant decreases in lipid peroxidation, which ultimately lead to a lower impact of Fe excess on the growth of plants amended with Si (Chalmardi et al., 2014; Dufey et al., 2014). Si has also been reported to reduce the Fe plaque formation in roots of rice plants challenged with Fe excess (Fu et al., 2012). Whether, or not, Si could prevent Fe toxicity on the photosynthesis and carbon metabolism remains elusive, however.

We here hypothesized that Si mitigates the effects of Fe toxicity on the photosynthetic performance and carbon metabolism of rice leaves, particularly in cultivars susceptible to Fe toxicity. To test this hypothesis we designed a greenhouse experiment using two rice cultivars with contrasting abilities to tolerate Fe toxicity; we challenged these cultivars with Fe excess and amended them with Si. Specifically, the following questions were addressed: (i) could silicon fertilization attenuate the Fe toxicity on the rice photosynthetic machinery? (ii) would Si be able to favor a metabolic homeostasis under conditions of Fe excess?

2. Materials and methods

2.1. Plant material, growth conditions and experimental design

The experiments were carried out in Viçosa (20°45′S, 42°54′W, 650 m above sea level) in south-eastern Brazil. Two lowland rice cultivars, BR-IRGA-409 and EPAGRI-109, respectively sensitive and tolerant to Fe excess (Stein et al, 2009, 2014) were used. Details of seed germination and early seedling growth have been described elsewhere (Dallagnol et al., 2011). The plants were grown in plastic pots (5 L volume) in a greenhouse with controlled air temperature (30/25 ± 2 °C (day/night)) and naturally fluctuating photosynthetic photon flux density (PPFD). The maximum PPFD values that were registered inside the greenhouse (approx. 70% of light transmittance) were *c.* 1500 μmol photons m^{-2} s^{-1}. The plants were grown in non-aerated culture solutions (pH adjusted daily to 5.0), prepared based on Hoagland and Arnon (1950), and included the following nutrients: 1.0 mM KNO_3; 0.25 mM $NH_4H_2PO_4$; 0.1 mM NH_4Cl; 0.5 mM $MgSO_4.7H_2O$; 1.0 mM $Ca(NO_3)_2$; 0.30 μM $CuSO_4.5H_2O$; 0.33 μM $ZnSO_4.7H_2O$; 11.5 μM H_3BO_3; 3.5 μM $MnCl_2.4H_2O$; 0.1 μM $(NH_4)_6Mo_7O_{24}.4H_2O$; 25 μM $FeSO_4.7H_2O$ and 25 μM EDTA bisodic. Si was supplied (2 mM) or not (0 mM) over the entire experiment as monosilicic acid, which was prepared by passing potassium silicate through cation-exchange resin (Amberlite IR-120B, H^+ form; Sigma-Aldrich, São Paulo, Brazil). Additionally, plants were divided into two groups: one received regular Fe supply (25 μM in the form of Fe-EDTA (FeSO4)) over the course of the experiment (control plants), and in the other group Fe was also supplied with 25 μM of Fe-EDTA until 45 days after transplanting, and then Fe supply was suddenly increased to 5 mM (Fe excess). This high Fe concentration corresponds to typical environmental conditions of Fe excess in relevant Brazilian rice producing areas (Stein et al., 2014). All the samplings and measurements were performed at 8 or 15 days after Fe excess additions (DAA). For biochemical analyses, leaf tissues were collected at midday, flash frozen in liquid nitrogen, and subsequently stored at −80 °C until required.

2.2. Fe and Si contents

Root and leaf tissues were previously washed in deionized water. Root materials were subsequently washed using a dithio-citrate-bicarbonate solution (DCB) for removing the Fe that was adsorbed to the tissues. This solution (1/4 strength), made with 40 mL of 0.3 M sodium citrate, 5 mL of 1 M sodium bicarbonate and 3 g of sodium dithionite (Taylor and Crowder, 1983), was prepared with chemicals (minimum purity of 99.5%) that were obtained from Sigma-Aldrich or Vetec (São Paulo, Brazil). Root tissues were maintained under constant shaking in DCB solutions during 3 h. Both root and leaf tissues were then oven-dried at 60 °C until constant mass and finely ground from which Fe was extracted by nitroperchloric digestion at 95 °C; Fe contents were subsequently determined using a SpectrAA 220 Fast Sequential AAS atomic absorption spectrometer (Varian, St. Clara, CA, USA) following Malavolta et al. (1989).

For Si analyses, plant tissues were washed in deionized water and then oven-dried at 60 °C until constant mass, after which they were ground to pass through a 40-mesh screen with a Thomas Wiley mill (Thomas Scientific, Swedesboro, NJ, USA). Si contents were colorimetrically determined on 0.1 g of dried and alkali-digested tissues (Dallagnol et al., 2011).

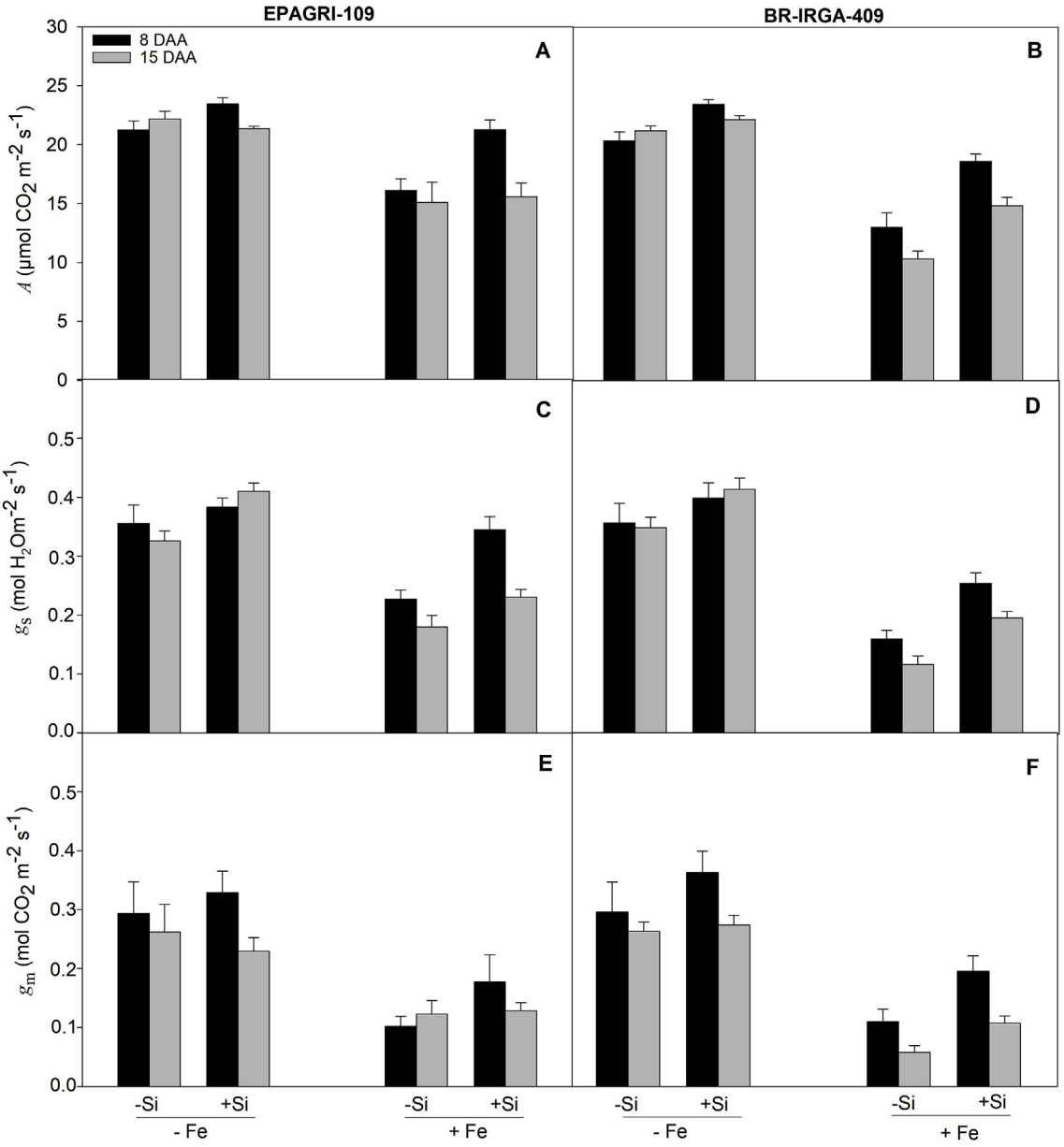

Fig. 2. The effects of silicon, Si (0 or 2 mM: Si or + Si, respectively), and iron, Fe (25 μM or 5 mM: Fe and +Fe, respectively), on the net CO_2 assimilation rate, *A* (A–B), stomatal conductance, g_s (C–D) and mesophyll conductance, g_m (E–F) of two rice cultivars [cv. 'EPAGRI-109' and cv. 'BR-IRGA-409', respectively tolerant and sensitive to Fe excess] grown in nutrient solutions. n = 5 ± SE.

2.3. Photosynthetic measurements

The leaf gas exchange parameters were assessed *in situ* in combination with measurements of Chl *a* fluorescence emission kinetics using two cross-calibrated open-flow gas exchange analysers (LI-6400XT, LI-COR, Lincoln, NE, USA) furnished with integrated fluorescence chamber heads (LI-6400-40, LI-COR Inc.). The net CO_2 assimilation rate (*A*), stomatal conductance to water vapor (g_s) and internal CO_2 concentration (C_i) were measured on attached, completely expanded leaves from 10:00 to 14:00 h (solar time), under artificial PPFD, *i.e.*, 1000 μmol m^{-2} s^{-1} at the leaf level and 400 μmol CO_2 mol^{-1} air. All measurements were performed at 25 °C, and the vapor pressure deficit was maintained at *c.*1.0 kPa; the amount of blue light was fixed to 10% of PPFD to optimize the stomatal aperture.

Segments from attached leaves were darkened for at least 30 min and then illuminated with weak modulated measuring beams (0.03 μmol m^{-2} s^{-1}) to obtain the initial fluorescence (F_0). Saturating white light pulses of 8000 μmol photons m^{-2} s^{-1} were employed for 0.8 s to warrant maximum Chl *a* fluorescence emissions (F_m), from which the variable-to-maximum Chl *a* fluorescence ratio, $F_v/F_m = [(F_m–F_0)/F_m)]$, was calculated. In light-adapted leaves, the steady-state fluorescence yield (F_s) was measured after computing the gas exchange variables. Subsequently, a saturating white light pulse (8000 μmol m^{-2} s^{-1}; 0.8 s) was applied to achieve the light-adapted maximum fluorescence (F_m'). The actinic light was then turned off, and far-red illumination was applied (2 μmol m^{-2} s^{-1}) to measure the light-adapted initial fluorescence (F_0'). The values of these variables were used to estimate the photochemical quenching coefficient (q_P) and the capture efficiency of excitation energy by open photosystem (PS) II reaction centres (F_v'/F_m') (Logan et al., 2007). The actual PSII photochemical efficiency (φ_{PSII}) was estimated as $\varphi_{PSII} = (F_m' – F_s)/F_m'$, as detailed elsewhere (Genty et al., 1989). The apparent electron transport rate (*J*) was estimated as $J = \Phi_{PSII}$*PPFD*β*α where β is a parameter associated with the partitioning of absorbed quanta between PS II and

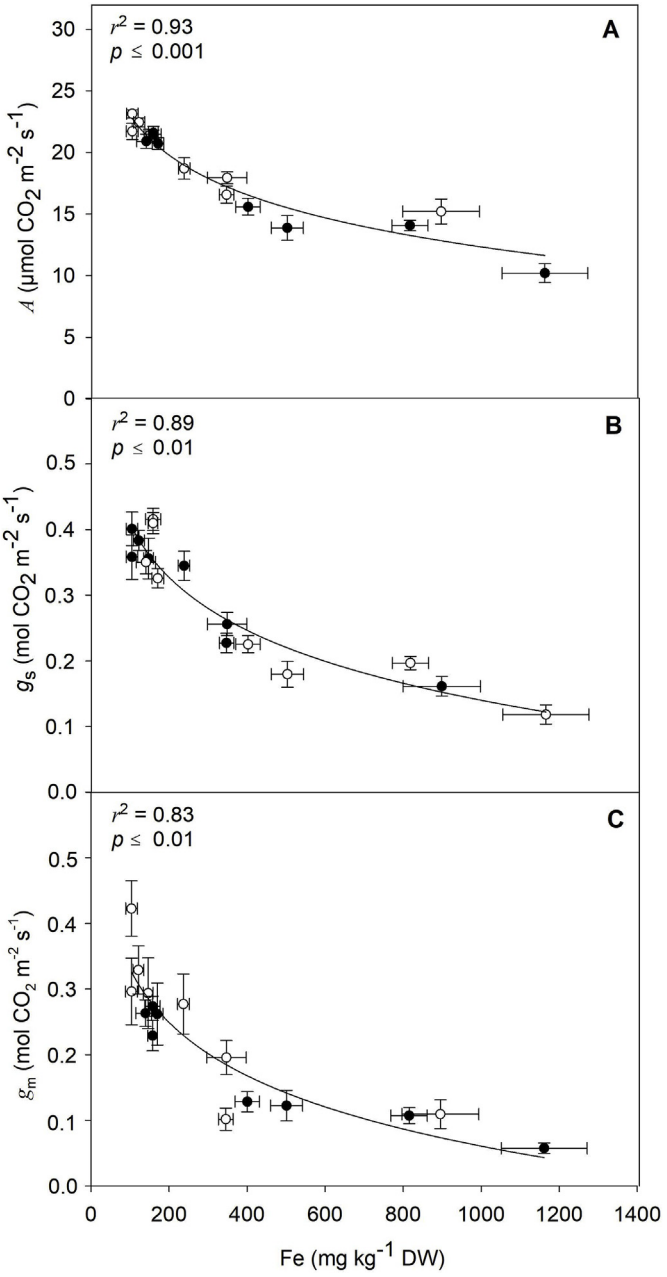

Fig. 3. The correlation between leaf iron (Fe) concentrations with the net CO_2 assimilation rate, *A* (A), stomatal conductance, g_s (B) and mesophyll conductance, g_m (C) of two rice cultivars [cv. 'EPAGRI-109' (open circles) and cv. 'BR-IRGA-409' (solid circles), respectively tolerant and sensitive to Fe excess] grown in nutrient solutions.

PS I and α is the leaf absorptance (Genty et al., 1989). The product of β and α was computed following the procedures of Valentini et al. (1995) under non-photorespiratory conditions.

The mitochondrial respiration rate in the light (R_l) was determined according to Martins et al. (2013) as the value that forces the intercept of the plot *A* versus C_i–C_c (chloroplastic CO_2 concentration) to be zero using points in the C_i range below 300 μmol mol^{-1} air (RuBisCO limitation).

The partitioning of electrons between photosynthesis (J_c) and photorespiration (J_o) was accomplished using the values of *J*, *A* and R_l, employing the equations outlined by Valentini et al. (1995) and Long and Bernacchi (2003).

To obtain *in situ* A/C_i curves, 4–5 plants per treatment were used. These curves were initiated at an ambient [CO_2] (C_a) of 400 μmol mol^{-1} air under a saturating PPFD of 1000 μmol m^{-2} s^{-1}. After reaching a steady state condition, C_a was progressively decreased to 50 μmol mol^{-1} air after which C_a was returned to 400 μmol mol^{-1} air to reestablish the original *A*. Next, C_a was increased stepwise to 1600 μmol mol^{-1} air. All of the gas exchange data were corrected for the leakage of CO_2 into and out of the leaf chamber of the LI-6400 as detailed in Rodeghiero et al. (2007).

Calculations of both C_c and mesophyll conductance to CO_2 (g_m) were performed using gas exchange and Chl *a* fluorescence variables according to the procedures outlined by Harley et al. (1992), and detailed in Detmann et al. (2012). The g_m values were used to convert A–C_i into A–C_c curves. These curves were then used to calculate the maximum carboxylation rate on a C_c basis (V_{cmax}) and the maximum carboxylation rate limited by electron transport (J_{max}) by fitting the mechanistic model of CO_2 assimilation as proposed by Farquhar et al. (1980) and detailed elsewhere (Martins et al., 2014); for these purposes, the C_c-based temperature dependence of the RuBisCO kinetic parameters were used (Bernacchi et al., 2002). The photosynthetic variables V_{cmax}, J_{max} and g_m were thereupon normalized to 25 °C following the temperature response equations described in Sharkey et al. (2007).

The overall photosynthetic limitations were fractionated into their functional components (stomatal, mesophyll and biochemical constraints) following the approach proposed by Grassi and Magnani (2005) and described in detail in Sanglard et al. (2014).

2.4. Metabolites

A 10-mg sample of lyophilized leaf tissue was finely ground and added to pure methanol, and the mixture was kept at 70 °C for 30 min. After an initial centrifugation(13,000 × *g*, 5 min), the pellets were extracted further two times using pure methanol. Supernatants were retained, combined, and stored at −20 °C for soluble sugar determinations. The concentrations of glucose, fructose and sucrose in the supernatants were measured through the reduction of NAD^+ by glucose-6-P dehydrogenase after the sequential addition of hexokinase, phosphoglucose isomerase and invertase, according to Trethewey et al. (1998); all of these chemicals were obtained from Sigma-Aldrich (São Paulo, Brazil), Reduction of NAD^+ was continuously registered at 340 nm using an ELISA reader (Tunable Microplate Reader,VERSAmax, Sunnyvale, USA). The pellet was suspended in KOH, incubated at 95 °C for 1 h, neutralized with acetic acid and centrifuged at 16,000 × *g* for 10 min. Starch was then hydrolyzed in 100 mM citrate buffer at pH 4.6 containing amyloglucosidase and _α-amylase (Trethewey et al., 1998), and the released glucose was assessed as described above. Proteins were also quantified from the methanol-insoluble pellet using bovine serum albumin as a standard (Bradford method). Further details have described elsewhere (Praxedes et al., 2006; Ronchi et al., 2006). The concentrations of malate and fumarate (from the methanol-soluble phase) were exactly determined as described elsewhere (Nunes-Nesi et al., 2007), using the above quoted ELISA reader.

Nucleotide extraction was performed by grinding lyophilized leaf materials in liquid nitrogen after which the appropriate extraction buffers were promptly added. First, 10 mg of lyophilized material were divided into two approximately equal samples to which 0.1 M $HClO_4$ or 0.1 M KOH was added. Two extracts were then obtained, one acidic (that was used for extracting oxidized $NAD(P)^+$), and another alkaline (that was used for extracting reduced NAD(P)H). Extracts were further neutralized by adding 0.1 M KOH 0.2 M Tris (pH = 8.4) on the acid extract or 0.1 M $HClO_4$ 0.2 M Tris (pH = 8.4) in the alkaline extract). NAD(H) content was assessed enzymatically in a medium containing 12 mM Na_2EDTA, 0.3 mM PES, 1.5 mM ethanol and alcohol dehydrogenase. NADP(H) was enzymatically quantified in a reaction medium containing 12 mM Na_2EDTA, 0.3 mM PMS, 1.8 mM MTT, 9 mM glucose-6-phosphate and the enzyme glucose-6-phosphate

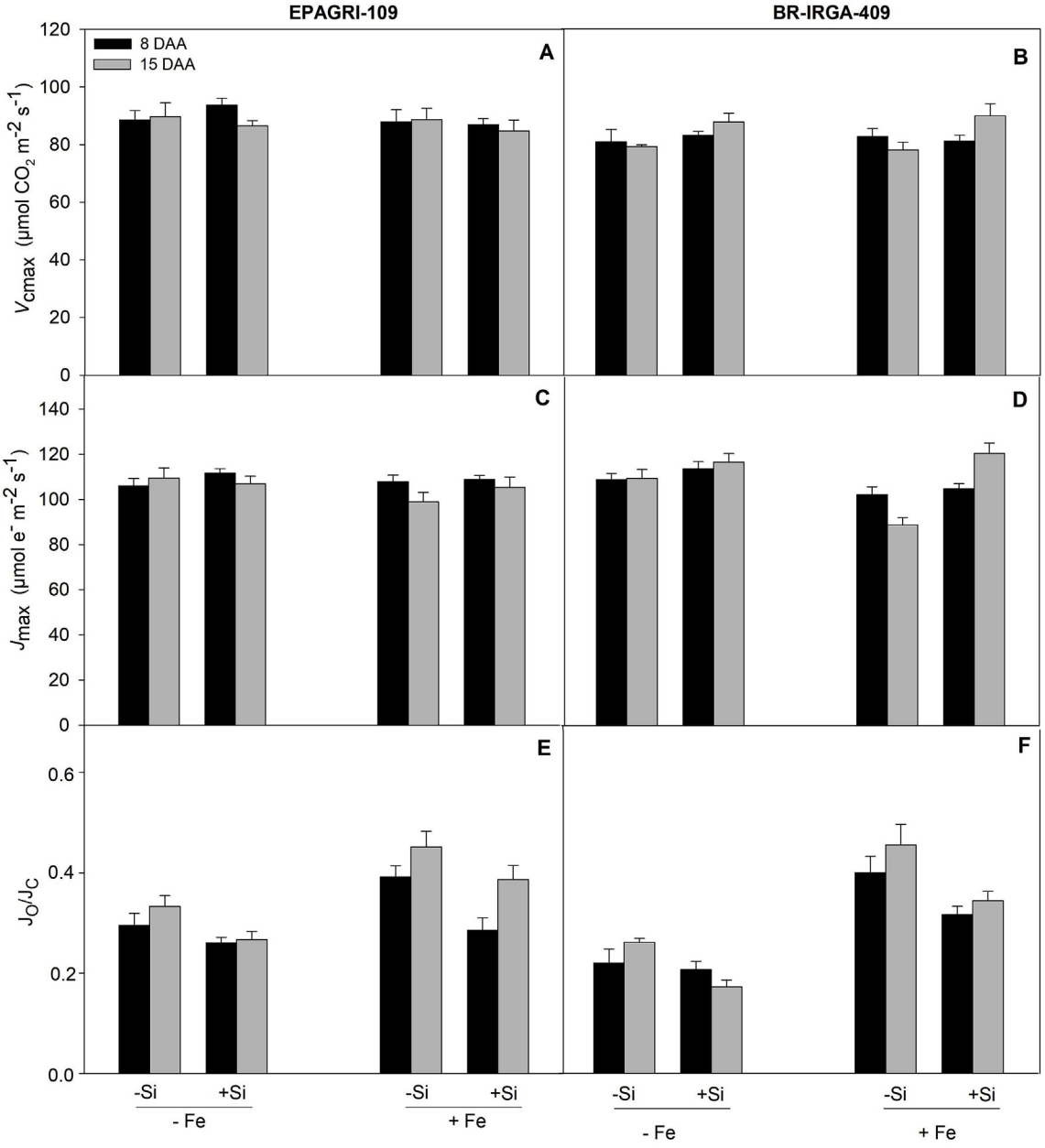

Fig. 4. The effects of silicon, Si (0 or 2 mM: Si or + Si, respectively), and iron, Fe (25 µM or 5 mM: Fe and +Fe, respectively), on the maximum rate of RuBisCO carboxylation on a chloroplast basis, V_{cmax} (A–B), maximum rate of carboxylation limited by electron transport, (J_{max} (C–D), and the ratio of electron transport rate devoted to oxygenation/carboxylation, J_o/J_c (E–F) of two rice cultivars [cv. 'EPAGRI-109' and cv. 'BR-IRGA-409', respectively tolerant and sensitive to Fe excess] grown in nutrient solutions. n = 5 ± SE.

dehydrogenase. Further details are given in Gibon et al. (2004).

2.5. Enzyme activities

Enzyme extracts were obtained from frozen leaf tissues as exactly described by Nunes-Nesi et al. (2007). Activities of citrate synthase, pyruvate kinase (PK), phosphoglycerate kinase (PGK) and ATP-dependent phosphofructokinase (ATP-PFK) were determined as described by Gibon et al. (2004); NAD-dependent malate dehydrogenase (NAD-MDH) and NADP-dependent isocitrate dehydrogenase (NADP-IDH) as by Jenner et al. (2001); aldolase, enolase, NAD-dependent glyceraldehyde-3-phosphate dehydrogenase (NAD-GAPDH) and triose-phosphate isomerase (TPI) as by Fernie et al. (2001); and acid and alkaline invertases and sucrose synthase (Susy) as reported in Praxedes et al. (2006). RuBisCO activity was assayed as described in Ronchi et al. (2006).

2.6. Statistical analysis

The experiment was arranged in a completely randomized design following a 2 × 2 × 2 factorial scheme (two genotypes x two Si levels x two Fe levels), with six plants in individual pots (48 in total) per each treatment serving as conditional replicates. The data were submitted to a three-way ANOVA with all main factors computed as fixed factors. The MIXED procedure of SAS (version 9.1) was used at an $\alpha = 0.05$. When any interaction was significant, the MIXED Slice statement was employed to analyse the dependency effect of the factors. Regression analysis was used to evaluate relationships between some selected traits.

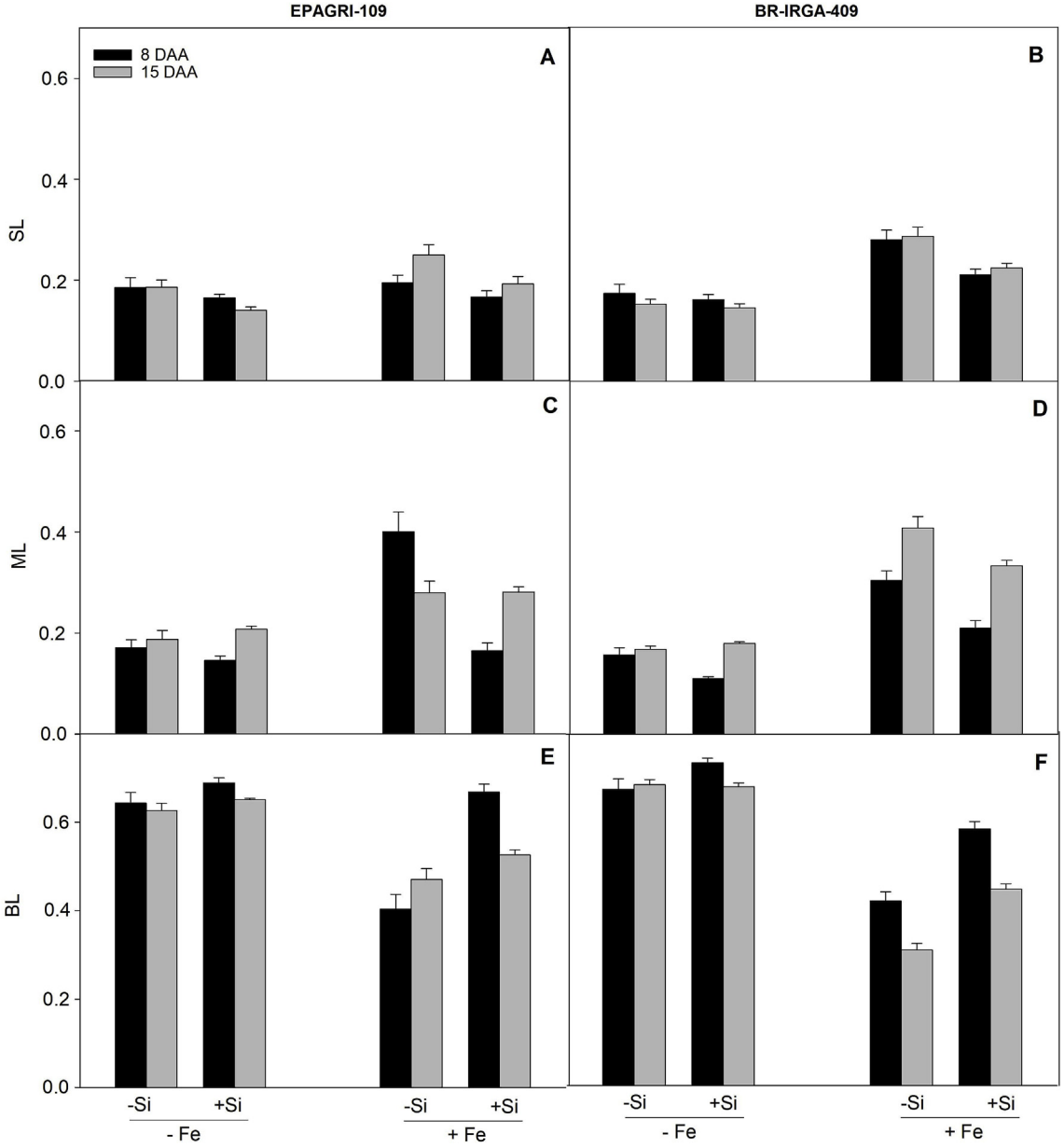

Fig. 5. The effects of silicon, Si (0 or 2 mM: Si or + Si, respectively), and iron, Fe (25 μM or 5 mM: Fe and +Fe, respectively), on the components of total limitations of photosynthesis: stomatal limitations, SL (A–B), mesophyll limitations, ML (C–D), and biochemical limitations, BL (E–F) of two rice cultivars [cv. 'EPAGRI-109' and cv. 'BR-IRGA-409', respectively tolerant and sensitive to Fe excess] grown in nutrient solutions. n = 5 ± SE.

3. Results

3.1. Si supply increases Si levels and decreases Fe levels, especially in the shoot

Regardless of cultivar, Si levels were higher in +Si plants, particularly in leaves relative to roots (Fig. 1A–D; Table 1). As expected, +Fe plants displayed remarkably higher Fe levels than their –Fe counterparts, as particularly noted in the Fe-sensitive cultivar (Fig. 1E–H; Table 1). In both cultivars, Fe contents increased over time. Presence of Si led to significantly decreased Fe levels in both leaves and roots, independently of cultivar and sampling dates (Fig. 1E–H; Table 1), and these decreases were more marked in the Fe-sensitive cultivar. Notably, the mitigating effects of Si resulted in greater reductions of Fe content in leaves than in roots (Fig. 1).

3.2. Si partially reverses the impairments of Fe excess on the photosynthetic rates by fundamentally affecting the leaf diffusive conductance with minimal changes in the photochemical and biochemical capacity

Fe toxicity led to reductions in A in accordance with decreases in both g_s and g_m (Fig. 2; Table 1). These reductions were more evident in the –Si plants, particularly in the Fe-sensitive cultivar. In fact, A, as well as g_s and g_m, correlated significantly ($r^2 \geq 0.83$) with leaf Fe contents (Fig. 3). The decreases in A due to Fe stress were partially reversed by Si, as observed at 8 or 15 DAA in the Fe-sensitive cultivar and also at 8 DAA in the Fe-tolerant cultivar (Fig. 2A and B; significant Si x Fe interaction, Table 1). Similar results were observed for g_s (Fig. 2C and D) and g_m (Fig. 2E and F). Interestingly, A correlated significantly with g_s ($r^2 = 0.96$) and g_m ($r^2 = 0.83$); also, g_s and g_m were linearly correlated to each other ($r^2 = 0.82$) (Supplementary Fig. 1).

The applied treatments affected minimally, if at all, the photochemical parameters (F_v/F_m, F_v'/F_m' and q_p) (Supplementary Fig. 2;

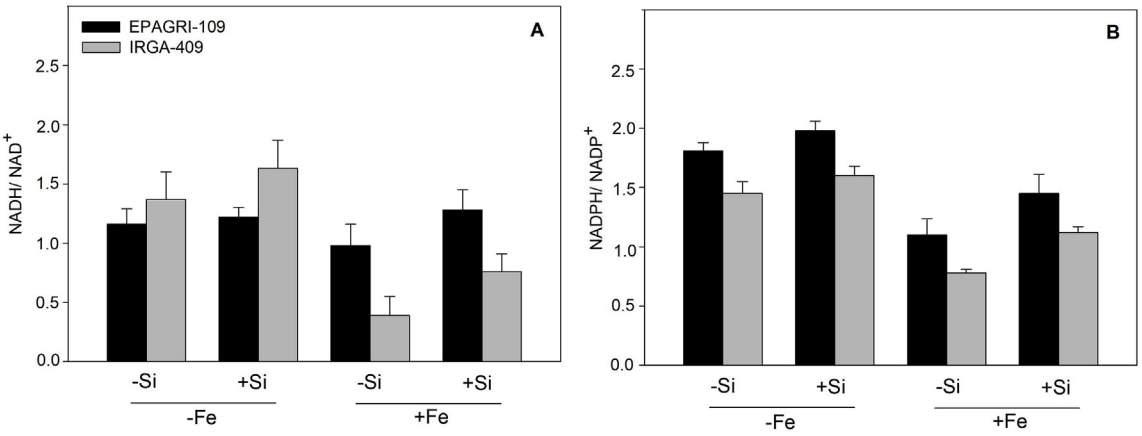

Fig. 6. The effects of silicon, Si (0 or 2 mM: Si or + Si, respectively), and iron, Fe (25 μM or 5 mM: Fe and +Fe, respectively), on the ratios of NADH/NAD$^+$ (A) and NADPH/NADP$^+$ (B) of two rice cultivars [cv. 'EPAGRI-109' and cv. 'BR-IRGA-409', respectively tolerant and sensitive to Fe excess] grown in nutrient solutions. n = 5 ± SE.

Table 1) as well as V_{cmax} (Fig. 4A and B) and J_{max} (Fig. 4 C-D). In contrast, there were effects of Si and Fe (significant Fe x Si interaction; Table 1) on the J_o/J_c ratio which increased more markedly in the Fe-sensitive cultivar under Fe excess; however, these increases were less pronounced in presence of Si (Fig. 4E and F). Taken together, these data are consistent with diffusion limitations of photosynthesis in response to the applied treatments, and support the linear relationship between A and C_c (r^2 = 0.89, Supplementary Fig. 1D).

3.3. Limitations to photosynthesis are impacted by Si/Fe

We next evaluated the functional components of the global limitations of photosynthesis. In–Fe plants, biochemical (BL) limitations accounted for most of the total photosynthetic constraints (67%) against approximately 16% for stomatal limitations (SL) and 17% for mesophyll limitations (ML), independently of cultivar (Fig. 5). In + Fe plants, SL were reduced regardless of cultivar and Fe stress duration with no effect of Si (Table 1, Fig. 5A and B). By contrast, Fe toxicity resulted in increased ML which were partially reversed by the addition of Si at 8 DAA in the Fe tolerant cultivar and at both 8 and 15 DAA in the sensitive cultivar (significant Si x Fe and Fe x Cv interactions, Table 1; Fig. 5C and D). The BL, in turn, were reduced in response to Fe toxicity (Fig. 5E and F), especially in –Si plants, independently of cultivar and stress duration (significant Si x Fe and Fe x Cv interactions). In summary, as can be deduced from Fig. 5, diffusional limitations (SL + ML) were responsible for approximately 60% of the total limitation of photosynthesis in +Fe plants, in contrast to their –Fe counterparts in which diffusional limitations did not exceed 40% of total photosynthetic limitations independently of Si application.

3.4. Carbon metabolism was minimally altered by the applied treatments

The activities of enzymes associated with carbon metabolism, including RuBisCO, responded little, if at all, to the treatments (Supplementary Fig. 3). Of the 16 enzymes analyzed, only three displayed a reduction in their catalytic activity in +Fe plants. However, these changes were relatively small and thus we suggest that Fe (and Si) had no major impact on central metabolism under the present experimental conditions. Overall, we were also unable to detect a mitigating effect of Si on the enzyme activities under Fe excess (Supplementary Fig. 3).

The NADH/NAD$^+$ and NADPH/NADP$^+$ ratios were decreased by 24% and 30% in –Si + Fe plants from the Fe-sensitive cultivar, and by 23% and 49% in the Fe-tolerant cultivar, respectively, when compared with their + Si + Fe counterparts (with no significant Si x Fe interaction) (Table 1, Fig. 6). In turn, glucose and fructose pools increased significantly in + Fe plants of both cultivars, but more markedly in –Si plants (Table 1, Fig. 7A and B). On the other hand, the concentrations of sucrose, starch and proteins were unaffected by the treatments (Table 1, Fig. 7C and D,G). Malate and fumarate concentrations increased under Fe toxicity, particularly in the Fe-sensitive cultivar; Si weakened these increases regardless of cultivar (significant Si x Fe interaction) (Table 1, Fig. 7E and F).

4. Discussion

Irrespective of cultivar, the levels of Fe in both leaves and roots of +Fe plants were above those that are considered critical for Fe toxicity (≥300–500 mg kg^{-1} dry mass) (Dobermann and Fairhurst, 2000). The Fe stress impaired the photosynthetic performance, particularly in the Fe-sensitive cultivar which displayed the highest leaf Fe levels. Notably, Si fertilization was associated with decreased Fe content and, as such, contributed to partially reverse the effects of Fe toxicity, in good agreement with our working hypothesis. It is also noted that Si per se did not affect A in –Fe plants, as also observed in other studies conducted with rice plants in their vegetative growth stage (Detmann et al., 2012; Sanglard et al., 2014).

Decreases in A in rice cultivars under Fe excess have been largely attributed to decreases in g_s (Pereira et al., 2013; Müller et al., 2015; Pinto et al., 2016). Here, we provided novel information that not only g_s but also g_m limits CO_2 flux towards the chloroplast stroma in response to Fe excess. Our results suggest an intrinsic correlation between g_s and g_m, as proposed by Flexas et al. (2008) and Flexas et al. (2012). Similar results have been obtained in rice in response to arsenic (Sanglard et al., 2014) and in sugar beet in response to zinc (Sagardoy et al., 2010). Given that the photochemical and biochemical abilities for CO_2 fixation were preserved under Fe excess, it is suggested that the reductions in A were mostly associated with diffusive limitations of photosynthesis.

The reduction of leaf conductance (g_s + g_m) in response to Fe excess (Fig. 2) was partially reversed by fertilization with Si. The reversal of these impacts depended on the time and exposure to Fe excess, being more evident at 8 than at 15 DAA, due possibly to the fact that Fe levels, more than the Si levels, increased over time irrespective of cultivar, as can be deduced from Fig. 1. Taken together, these results suggest that the mitigating effects of Si on Fe excess could be fundamentally associated with the reduction of Fe levels in + Si plants, in good agreement with the sharp relationships between A, g_s and g_m with leaf Fe concentrations. In any case we cannot dismiss some direct effect of Si on g_s and/or g_m (significant Si effects, Table 1). Although the physiological mechanisms associated with these effects have not been established,

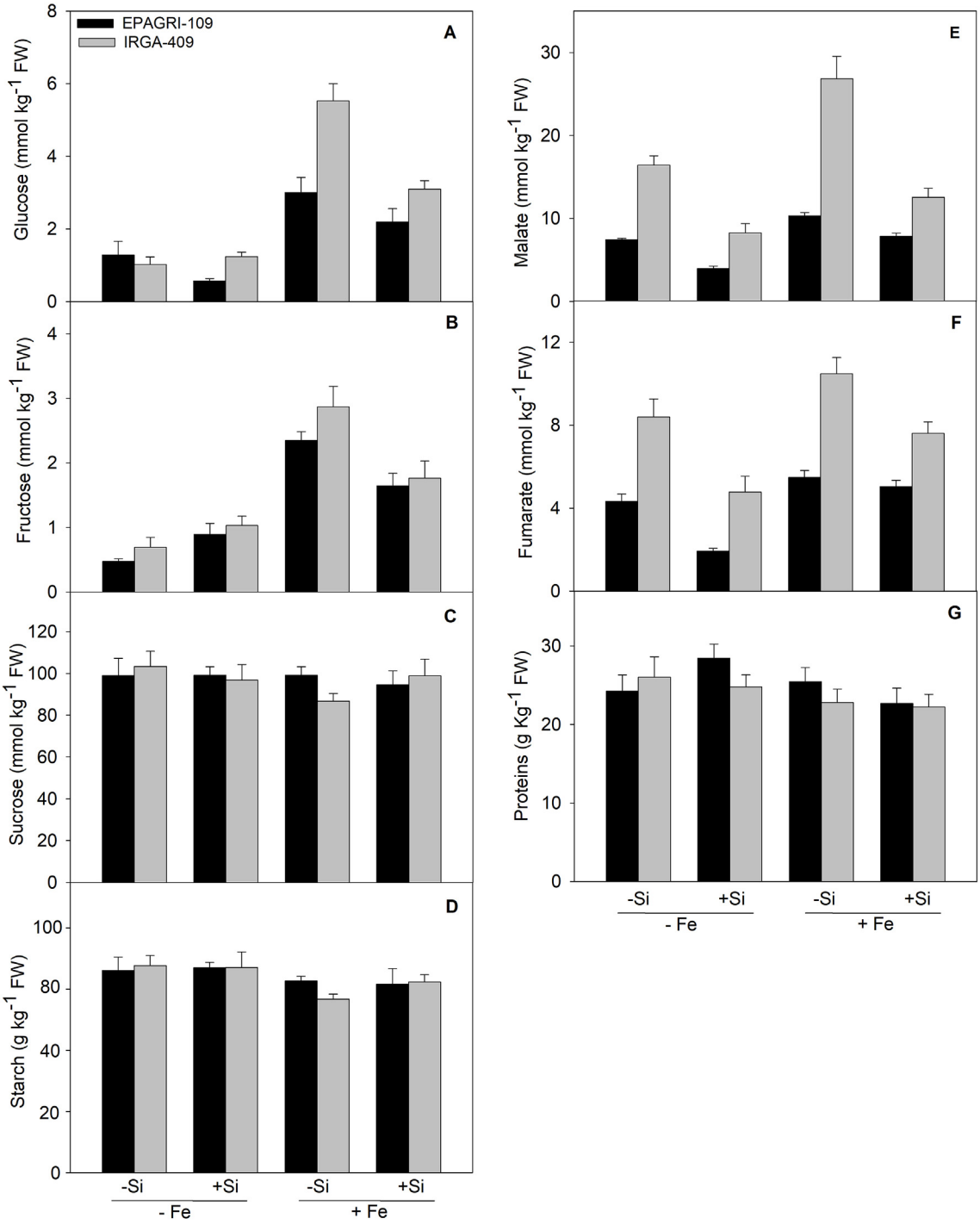

Fig. 7. The effects of silicon, Si (0 or 2 mM: Si or + Si, respectively), and iron, Fe (25 μM or 5 mM: Fe and +Fe, respectively), on the leaf concentrations of glucose (A), fructose (B), sucrose (C), starch (D), malate (E), fumarate (F) and proteins (G) of two rice cultivars [cv. 'EPAGRI-109' and cv. 'BR-IRGA-409', respectively tolerant and sensitive to Fe excess] grown in nutrient solutions. n = 5 ± SE.

some evidence suggests that Si may directly affect photosynthesis via modulating g_s (Lavinsky et al., 2016) or g_m (Detmann et al., 2012) in rice plants in the reproductive phase under unstressed conditions.

We obtained compelling evidence suggesting that the effects of Fe stress on *A* were, to a great extent, unrelated to photochemical or biochemical constraints of photosynthesis. First, our analysis of Chl *a* fluorescence demonstrated minimal variations, if any, in both the maximum PSII photochemical efficiency (F_v/F_m) and the photochemical quenching coefficient (q_P), suggesting stability of photochemical reactions in +Fe plants; these results contrast with those from other studies (e.g., Kampfenkel et al., 1995; Suh et al., 2002; Onyango et al., 2019) which have reported a higher susceptibility of PSII reaction centres to photoinhibition under Fe stress. Second, J_{max} was kept at high values, even when *A* was severely impaired, suggesting that the synthesis of both ATP and NADPH required to drive CO_2 fixation was largely uncompromised in +Fe plants. Third, the lack of treatment effect on V_{cmax} implies that the RuBisCO capacity to fix CO_2 was preserved, in good agreement with unresponsiveness of RuBisCO activity to Fe excess. In any case, because both F_v/F_m and F_v'/F_m' (a proxy for thermal dissipation; Logan et al., 2007) were relatively invariant to the treatments

we applied, we contend that modification/inactivation of the PSII reaction centers and photoprotection by xanthophylls engaged in sustained thermal energy dissipation may have been unlikely (Logan et al., 2007) under our experimental conditions. Given that the J_o/J_c ratio tended to increase under Fe stress (particularly in –Si plants), we suggest that photorespiration should have played a key role for dissipating excess energy. Other energy dissipation mechanisms, such as the water-water cycle (Asada, 2000) or cyclic flow of electrons within PSII (Heber et al., 2001), could also have played a role in dissipating the excess reducing power under Fe stress, which seems to be consistent with the observed reductions in $NADH/NAD^+$ and $NADPH/NADP^+$ ratios.

Accumulation of metabolites such as hexoses (glucose and fructose) is commonly observed under conditions of abiotic stress, although it varies with the time and extent of stress imposed (Radomiljac et al., 2013; Sanglard et al., 2016), as observed here under Fe toxicity. In *Arabidopsis thaliana* some studies have reported that sugar levels increase remarkably under abiotic stress, which have usually been associated with osmorregulation, membrane stabilization and protection, and altered carbon balance conditions (Rizhsky et al., 2004; Kaplan et al., 2007; Hummel et al., 2010). In addition, accumulation of organic acids (malate and fumarate) in both cultivars under Fe excess may be related to the non-cyclic functioning of the mitochondrial tricarboxylic acid cycle, or alterations in cell redox balance (Hummel et al., 2010; Igamberdiev and Eprintsev, 2016). Nonetheless, the levels of hexoses were much lower than those of sucrose + starch (which remained unaltered regardless of treatments), thus concurring for an invariant concentration of non-structural carbohydrates. This fact may be associated with the lower demand for assimilates in the +Fe plants, which accumulated less biomass than their –Fe counterparts (data not shown).

In conclusion, we here demonstrated that Si fertilization was able to partially reverse the toxic effects of Fe on the photosynthesis by fundamentally reducing the accumulation of Fe in the leaf tissues. This seems to largely explain the lower Fe content in +Si plants associated with higher g_s and g_m values, thus contributing to mitigate the negative impacts of Fe excess on A in +Si + Fe plants. Notably, Fe toxicity and/or Si fertilization affected minimally the photochemistry and biochemistry of photosynthesis; these facts, coupled with little, if at all, alterations of enzyme activities associated with the central carbon metabolism, suggest a remarkable metabolic homeostasis under Fe toxicity. It remains to be investigated the underlying mechanisms by which Fe at excess levels impairs leaf conductance and thus the magnitude of photosynthetic rates.

Author contributions

M. Santos performed the experiments and data analyses, and prepared the graphs and tables. L. Sanglard, M. Barbosa, D. Melo and W. Gonzafa performed the experiments. S. Martins helped in data analyses and helped to write the paper. F. DaMatta designed the experiment and wrote the paper.

Conflicts of interest

The authors hereby declare no conflicts of interests.

Acknowledgements

This research was supported by the Foundation for Research Assistance of Minas Gerais State, Brazil (FAPEMIG), Grant (CRA-APQ-02132-15) and by the National Council for Scientific and Technological Development, Brazil (CNPq), Grant (308652/2014-2) granted to FMD. This study was also financed in part by the Brazilian Federal Agency for Support and Evaluation of Graduate, Brazil (CAPES), Finance Code (001). Thanks are due also to the Instituto Riograndense do Arroz (IRGA) and Empresa de Pesquisa Agropecuária e Extensão Rural de Santa Catarina (EPAGRI) which kindly supplied the rice seeds.

Appendix A. Supplementary data

Supplementary data to this article can be found online at https://doi.org/10.1016/j.plaphy.2019.09.011.

References

Audebert, A., Fofana, M., 2009. Rice yield gap due to iron toxicity in West Africa. J. Agron. Crop Sci. 195, 66–76.
Asada, K., 2000. The water–water cycle as alternative photon and electron sinks. Philos. Trans. R. Soc. Lond. B: Biol. Sci. 355, 1419–1431.
Bernacchi, C.J., Portis, A.R., Nakano, H., von Caemmerer, S., Long, S.P., 2002. Temperature response of mesophyll conductance. Implications for the determination of rubisco enzyme kinetics and for limitations to photosynthesis *in vivo*. Plant Physiol. 130, 1992–1998.
Chalmardi, Z.C., Abdolzadeh, A., Sadeghipour, H.K., 2014. Silicon nutrition potentiates the antioxidant metabolism of rice plants under iron toxicity. Acta Physiol. Plant. 36, 493–502.
Coskun, D., Deshmukh, R., Sonah, H., Menzies, J.G., Reynolds, O., Ma, J.F., Kronzucker, H.J., Bélanger, R.R., 2019. The controversies of silicon's role in plant biology. New Phytol. 221, 67–85.
Dallagnol, L.J., Rodrigues, F.A., DaMatta, F.M., Mielli, M.V.B., Pereira, S.C., 2011. Deficiency in silicon uptake affects cytological, physiological, and biochemical events in the rice *Bipolaris oryzae* interaction. Phytopathology 101, 92–104.
Debona, D., Rodrigues, F.A., Datnoff, L.E., 2017. Silicon's role in abiotic and biotic plant stresses. Annu. Rev. Phytopathol. 55, 1–23.
Detmann, K.C., Araújo, W.L., Martins, S.C.V., Sanglard, L.M.V.P., Reis, J.V., Detmann, E., Rodrigues, F.A., Nunes-Nesi, A., Fernie, A.R., DaMatta, F.M., 2012. Silicon nutrition increases grain yield, which, in turn, exerts a feed-forward stimulation of photosynthetic rates via enhanced mesophyll conductance and alters primary metabolism in rice. New Phytol. 196, 752–762.
Dobermann, A., Fairhurst, T., 2000. Rice: Nutrient Disorders and Nutrient Management. International Rice Research Institute, Manila, Philippines.
Dufey, S.G., Ingabire, A., Lutts, S., Bertin, P., 2014. Silicon application in cultivated rices (*Oryza sativa* L and *Oryza glaberrima* Steud) alleviates iron toxicity symptoms through the reduction in iron concentration in the leaf tissue. J. Agron. Crop Sci. 200, 132–142.
Farquhar, G.D., von Caemmerer, S., Berry, J.A., 1980. A biochemical model of photosynthetic CO_2 assimilation in leaves of C3 species. Planta 149, 78–90.
Fernie, A.R., Roscher, A., Ratcliffe, R.G., Kruger, N.J., 2001. Fructose 2,6-bisphosphate activates pyrophosphate: fructose-6-phosphate 1-phosphotransferase and increases triose phosphate to hexose phosphate cycling in heterotrophic cells. Planta 212, 250–263.
Flexas, J., Ribas-Carbó, M., Díaz-Espejo, A., Galmés, J., Medrano, H., 2008. Mesophyll conductance to CO_2: current knowledge and future prospects. Plant Cell Environ. 31, 602–621.
Flexas, J., Barbour, M.M., Brendel, O., Cabrera, H.M., Carriquí, M., Díaz-Espejo, A., Douthec, C., Dreyerc, E., Ferrio, J.P., Gagoa, J., Gallé, A., Galmés, J., Kodama, N., Medrano, H., Niinemets, U., Peguero-Pina, J.J., Pou, A., Ribas-Carbó, M., Tomás, M., Tosens, T., Warren, C.R., 2012. Mesophyll diffusion conductance to CO_2: an unappreciated central player in photosynthesis. Plant Sci. 193, 70–84.
Fu, Y.-Q., Shen, H., Wu, D.-M., Cai, K.-Z., 2012. Silicon-mediated amelioration of Fe^{2+} toxicity in rice (*Oryza sativa* L.) roots. Pedosphere 22, 795–802.
Genty, B., Briantais, J.M., Baker, N.R., 1989. The relationship between the quantum yield of photosynthetic electron-transport and quenching of chlorophyll fluorescence. Biochim. Biophys. Acta 990, 87–92.
Gibon, Y., Blaesing, O.E., Hannemann, J., Carillo, P., Höhne, M., Hendriks, J.H.M., Palacios, N., Cross, J., Selbig, J., Stitt, M., 2004. A robot-based platform to measure multiple enzyme activities in *Arabidopsis* using a set of cycling assays: comparison of changes of enzyme activities and transcript levels during diurnal cycles and in prolonged darkness. Plant Cell 16, 3304–3325.
Grassi, G., Magnani, F., 2005. Stomatal, mesophyll conductance and biochemical limitations to photosynthesis as affected by drought and leaf ontogeny in ash and oak trees. Plant Cell Environ. 28, 834–849.
Gunes, A., Inal, A., Bagci, E.G., Coban, S., Pilbeam, D.J., 2007. Silicon mediates changes to some physiological and enzymatic parameters symptomatic for oxidative stress in spinach (*Spinacia oleracea* L.) grown under B toxicity. Sci. Hortic. 113, 113–119.
Harley, P.C., Loreto, F., Di Marco, G., Sharkey, T.D., 1992. Theoretical considerations when estimating mesophyll conductance to CO_2 flux by analysis of the response of photosynthesis to CO_2. Plant Physiol. 98, 1429–1436.
Heber, U., Bulhov, N.G., Shuvalov, V.A., Kobayashi, Y., Lange, O.L., 2001. Protection of the photosynthetic apparatus against damage by excessive illumination in homoiohydric leaves and poikilohydric mosses and lichens. J. Exp. Bot. 363, 199–2006.
Hummel, I., Pantin, F., Sulpice, R., Piques, M., Rolland, G., Dauzat, M., Dauzat, M., Christophe, A., Pervent, M., Bouteillé, M., Stitt, M., Gibon, Y., Müller, B., 2010. Arabidopsis plants acclimate to water deficit at low cost through changes of carbon usage: an integrated perspective using growth, metabolite, enzyme, and gene expression analysis. Plant Physiol. 154, 357–372.
Hoagland, D.R., Arnon, D.I., 1950. The Water Culture Method for Growing Plants without Soils. California Agricultural Experimental Station, Berkeley, USA.
Igamberdiev, A.U., Eprintsev, A.T., 2016. Organic acids: the pools of fixed carbon involved in redox regulation and energy balance in higher plants. Front. Plant Sci. 7, 1042.
Jenner, H.L., Winning, B.M., Millar, A.H., Tomlinson, K.L., Leaver, C.J., Hill, S.A., 2001.

NAD malic enzyme and the control of carbohydrate metabolism in potato tubers. Plant Physiol. 126, 1139–1149.
Kampfenkel, K., Van, M.V., Inze, D., 1995. Extraction and determination of ascorbate and dehydroascorbate from plant tissue. Anal. Biochem. 225, 165–167.
Kaplan, F., Kopka, J., Sung, D.Y., Zhao, W., Popp, M., Porat, R., Guy, C.L., 2007. Transcript and metabolite profiling during cold acclimation of *Arabidopsis* reveals an intricate relationship of cold-regulated gene expression with modifications in metabolite content. Plant J. 50 967-9812007.
Lavinsky, A.O., Detmann, K.C., Reis, J.V., Ávila, R.T., Sanglard, M.L., Pereira, L.F., Sanglard, L.M.V.P., Rodrigues, F.A., Araújo, W.L., DaMatta, F.M., 2016. Silicon improves rice grain yield and photosynthesis specifically when supplied during the reproductive growth stage. J. Plant Physiol. 206, 125–132.
Li, P., Song, A., Li, Z., Fan, F., Liang, Y., 2012. Silicon ameliorates manganese toxicity by regulating manganese transport and antioxidant reactions in rice (*Oryza sativa* L.). Plant Soil 354, 407–419.
Liang, Y., Yang, C., Shi, H., 2001. Effects of silicon on growth and mineral composition of barley grown under toxic levels of aluminium. J. Plant Nutr. 24, 229–242.
Logan, B.A., Adams, W.W., Demmig-Adams, B., 2007. Avoiding common pitfalls of chlorophyll fluorescence analysis under field conditions. Funct. Plant Biol. 34, 853–859.
Long, S.P., Bernacchi, C.J., 2003. Gas exchange measurements, what can they tell us about the underlying limitations to photosynthesis? Procedures and sources of error. J. Exp. Bot. 54, 2393–2401.
Malavolta, E., Vitti, G.C., Oliveira, S.A., 1989. Evaluation of the Nutritional State of Plants: Principles and Applications. Potafos, Piracicaba, Brazil.
Martins, S.C.V., Galmés, J., Cavatte, P.C., Pereira, L.F., Ventrella, M.C., DaMatta, F.M., 2014. Understanding the low photosynthetic rates of sun and shade coffee leaves: bridging the gap on the relative roles of hydraulic, diffusive and biochemical constraints to photosynthesis. PLoS One 9, e95571.
Martins, S.C.V., Galmés, J., Molins, A., DaMatta, F.M., 2013. Improving the estimation of mesophyll conductance: on the role of electron transport rate correction and respiration. J. Exp. Bot. 64, 3285–3298.
Müller, C., Kuki, K.N., Pinheiro, D.T., Souza, L.R.S., Silva, A.I.S., Loureiro, M.E., Oliva, M.A., Almeida, A.M., 2015. Differential physiological responses in rice upon exposure to excess distinct iron forms. Plant Soil 391, 123–138.
Neumann, D., zur Nieden, U., 2001. Silicon and heavy metal tolerance of higher plants. Phytochemistry 56, 685–692.
Nunes-Nesi, A., Carrari, F., Gibon, Y., Sulpice, R., Lytovchenko, A., Fisahn, J., Graham, J., Ratcliff, R.G., Sweetlove, L.J., Fernie, A.R., 2007. Deficiency of mitochondrial fumarase activity in tomato plants impairs photosynthesis via an effect on stomatal function. Plant J. 50, 1093–1106.
Onaga, G., Dramé, K.N., Ismail, A.M., 2016. Understanding the regulation of iron nutrition: can it contribute to improving iron toxicity tolerance in rice? Funct. Plant Biol. 43, 709–726.
Onyango, D.A., Entila, F., Dida, M.M., Ismail, A.M., Drame, K.N., 2019. Mechanistic understanding of iron toxicity tolerance in contrasting rice varieties from Africa: 1. Morpho-physiological and biochemical responses. Funct. Plant Biol. 46, 93–105.
Pereira, E.G., Oliva, M.A., Rosado-Souza, L., Mendes, G.C., Colares, D.S., Stopato, C.H., Almeida, A.M., 2013. Iron excess affects rice photosynthesis through stomatal and non-stomatal limitations. Plant Sci. 201–202, 81–92.
Pereira, E.G., Oliva, M.A., Siqueira-Silva, A.I., Rosado-Souza, L., Pinheiro, D.T., Almeida, A.M., 2014. Tropical rice cultivars from lowland and upland cropping systems differ in iron plaque formation. J. Plant Nutr. 37, 1373–1394.
Pinto, S.S., Souza, A.E., Oliva, M.A., Pereira, E.G., 2016. Oxidative damage and photosynthetic impairment in tropical rice cultivars upon. Sci. Agric. 73, 217–226.
Praxedes, S.C., DaMatta, F.M., Loureiro, M.E., Ferrão, M.A.G., Cordeiro, A.T., 2006. Effects of long-term soil drought on photosynthesis and carbohydrate metabolism in mature robusta coffee (*Coffea canephora* Pierre var. *kouillou*) leaves. Environ. Exp. Bot. 56, 263–273.
Radomiljac, J.D., Whelan, J., Merwe, M.V.D., 2013. Coordinating metabolite changes with our perception of plant abiotic stress responses: emerging views revealed by integrative- omic analyses. Metabolites 3, 761–786.
Ricachenevsky, F.K., Sperotto, R.A., Menguer, P.K., Fett, J.P., 2010. Identification of Fe-excess-induced genes in rice shoots reveals a WRKY transcription factor responsive to Fe, drought and senescence. Mol. Biol. Rep. 37, 3735–3745.
Rizhsky, L., Liang, H., Shuman, J., Shulaev, V., Davletova, S., Mittler, R., 2004. When defense pathways collide. The response of *Arabidopsis* to a combination of drought and heat stress. Plant Physiol. 134, 1683–1696.
Rodeghiero, M., Niinemets, Ü., Cescatti, A., 2007. Major diffusion leaks of clamp-on leaf cuvettes still unaccounted: how erroneous are the estimates of Farquhar et al, model parameters? Plant Cell Environ. 30, 1006–1022.
Ronchi, C.P., DaMatta, F.M., Batista, K.D., Moraes, G.A.B.K., Loureiro, M.E., Ducatti, C., 2006. Growth and photosynthetic down-regulation in *Coffea arabica* in response to restricting root volume. Funct. Plant Biol. 33, 1013–1023.
Sanglard, L.M.V.P., Martins, S.C.V., Detmann, K.C., Silva, P.E.M., Lavinsky, A.O., Silva, M.M., Detmann, E., Araújo, W.L., DaMatta, F.M., 2014. Silicon nutrition alleviates the negative impacts of arsenic on the photosynthetic apparatus of rice leaves: an analysis of the key limitations of photosynthesis. Physiol. Plant. 152, 355–366.
Sanglard, L.M.V.P., Detmann, K.C., Martins, S.C.V., Teixeira, R.A., Pereira, L.F., Sanglard, M.L., Fernie, A.R., Araújo, W.L., DaMatta, F.M., 2016. The role of silicone in metabolic acclimation of rice plants challenged with arsenic. Environ. Exp. Bot. 123, 22–36.
Sagardoy, R., Vázquez, S., Florez-Sarasa, I.D., Albacete, A., Ribas-Carbó, M., Flexas, J., Abadía, J., Morales, F., 2010. Stomatal and mesophyll conductances to CO_2 are the main limitations to photosynthesis in sugar beet (B*eta vulgaris)* plants grown with excess zinc. N*ew Phytol* 1**87**, 145–158.
Shi, G., Cai, Q., Liu, C., Wu, L., 2010. Silicon alleviates cadmium toxicity in peanut plants in relation to cadmium distribution and stimulation of antioxidative enzymes. Plant Growth Regul. 61, 45–52.
Siedlecka, A., Krupa, Z., Samuelsson, G., Öquist, G., Gardeström, 1997. Primary carbon metabolism in *Phaseolus vulgaris* plants under Cd(II)/Fe interaction. Plant Physiol. Biochem. 35, 951–957.
Silveira, C.V., Oliveira, A.P., Sperotto, R.A., Espindola, L.S., Amaral, L., Dias, J.F., Cunha, J.B., Fett, J.P., 2007. Influence of iron on mineral status of two rice (*Oryza sativa* L.) cultivars. Braz. J. Plant Physiol. 19, 127–139.
Sharkey, T.D., Bernacchi, C.J., Farquhar, G.D., Singsaas, E.L., 2007. Fitting photosynthetic carbon dioxide response curves for C3 leaves. Plant Cell Environ. 30, 1035–1040.
Stein, R.J., Duarte, G.L., Spohr, M.G., Lopes, S.I.G., Fett, J.P., 2009. Distinct physiological responses of two rice cultivars subjected to iron toxicity under field conditions. Ann. Appl. Biol. 154, 269–277.
Stein, R.J., Lopes, S.I.G., Fett, J.P., 2014. Iron toxicity in field-cultivated rice: contrasting tolerance mechanisms in distinct cultivars. Theor. Exp. Plant Physiol. 26, 135–146.
Suh, H.J., Kim, C.S., Lee, J.Y., Jung, J., 2002. Photodynamic effect of iron excess on photosystem II function in pea plants. Photochem. Photobiol. 75, 513–518.
Taylor, G.J., Crowder, A.A., 1983. Use of the DCB technique for extraction of hydrous iron oxides from roots of wetland plants. Am. J. Bot. 70, 1254–1257.
Trethewey, R.N., Geigenberger, P., Riedel, K., Hajirezaei, M.R., Sonnewald, U., Stitt, M., Reismeier, J.W., Willmitzer, L., 1998. Combined expression of glucokinase and invertase in potato tubers leads to a dramatic reduction in starch accumulation and a stimulation of glycolysis. Plant J. 15, 109–118.
Valentini, R., Epron, D., Angelis, P., Matteucci, G., Dreyer, E., 1995. *In situ* estimation of net CO_2 assimilation, photosynthetic electron flow and photorespiration in Turkey oak (*Q. cerris* L.) leaves: diurnal cycles under different levels of water supply. Plant Cell Environ. 18, 631–640.
Velikova, V., Tsonev, T., Loreto, F., Centritto, M., 2011. Changes in photosynthesis, mesophyll conductance to CO_2, and isoprenoid emissions in *Populus nigra* plants exposed to excess nickel. Environ. Pollut. 159, 1058–1066.
Vigani, G., Zocchi, G., Bashir, K., Philippar, K., Briat, J.F., 2013. Signals from chloroplasts and mitochondria for iron homeostasis regulation. Trends Plant Sci. 18, 305–311.